

Modelling Studies of Retrofitted Anchorage System in Exterior Beam Column Joint by Supplementary Steel

Padmanabham, K^{1*}, Rambabu, K², Sairam, K³

¹Ph.D Research Scholar, Civil Engineering Department, Andhra University, Visakhapatnam, India

²Professor, Civil Engineering Department, Andhra University, Visakhapatnam, India

³M.Tech, Civil Engineering Department, Gayatri Vidya Parishad (A), Visakhapatnam, India

DOI: [10.36348/sjce.2022.v06i09.001](https://doi.org/10.36348/sjce.2022.v06i09.001)

| Received: 28.07.2022 | Accepted: 01.09.2022 | Published: 04.09.2022

*Corresponding author: Padmanabham, K

Ph.D Research Scholar, Civil Engineering Department, Andhra University, Visakhapatnam, India

Abstract

A Nonlinear finite element based ABAQUS modeling studies were conducted to evaluate the performance of exterior Beam Column Joint (BCJ) under quasi-static test loads. Six integrated BCJ models representing different configurations of beam reinforcement anchored in joint are verified by using a novel retrofitting technique called "Post Installation of Supplementary Anchorage" (PISA) by using headed bar as supplementary steel. The configuration of beam reinforcement anchored in column are described by straight bar, 90 degree bend, 180 degree hook (confirming to design code IS456:2000) and single head, double head bars (confirming to ACI 318-19, ACI 352R-02) and 90 degree long bend of ductile detailing (as per IS 13920-2016). Two series (A&B) of integrated joint specimens representing conventional (series-A) and retrofitted anchorage (series-B) systems are modeled and tested by using ABAQUS software. The test parameters considered are configuration of anchorage system and presence of supplementary anchorage. The test variables representing nonlinear performance of retrofitted joint system are Von Mises stress conditions, Principal tensile stress, Moment-Rotation, Degraded stiffness, Crack mechanics and Damage index. The results shows good improvement of post failure conditions of exterior beam-column joint such as relocation of plastic hinge mechanism and failure mechanics of retrofitted joint system. Also the results validated with experimental program on typical specimens casted and tested. This study imparts useful information on implicit retrofitting methods applied by external means in exterior beam-column joint. It also promotes performance based design principles with viable construction practice.

Keywords: Beam column joint, Supplementary Anchorage, ABAQUS modeling, configuration of Anchorage, Post Retrofitting.

Copyright © 2022 The Author(s): This is an open-access article distributed under the terms of the Creative Commons Attribution **4.0 International License (CC BY-NC 4.0)** which permits unrestricted use, distribution, and reproduction in any medium for non-commercial use provided the original author and source are credited.

1. INTRODUCTION

The performance of RC framed structures are significantly influenced by integrity of joints or structural connections of beam-column joints since they are considered as one of the critical region in RC framed system. Most of the RC beam-column joints are lead to brittle failures and causes severe damages in the global structure. The design assumptions of strong column and weak beam with rigid joint conditions are unable to sustain during peak load conditions of high shear, and axial forces generated in the integrated joint region. In most of the design practice the beam-column joints are considered to be rigid in nature and the members meeting at a joint deform (rotate) by the same angle. But in real practice, joints are unable to sustain with force-deformation characteristics and not promote satisfactory levels of serviceability conditions. Post-

earthquake analysis of seismic structures and distress by impact or accidental loads in joint core are more prominent in RC framed structures. To improve the safety levels of global structure under sustained static and impact loads, the structure must able to resist high shear and ductility of beam-column joint. As per the design norms the plastic hinge mechanism should appear in beams rather than joint core. This design philosophy is called as "Strong column –Weak beam" theory with due considerations of shear deformation. In order to meet the ductility requirements, the detailing aspects of anchorage system in joint core of beam-column joint should meet the requirements of design standards mentioned in various codes (ACI, NZS, AIJ).

In reinforced concrete structure, the load is not applied directly on reinforcement, but acts on concrete

(Park and Paulay, 1974). The reinforcement can receive its share of load only when the load is transferred to it from the concrete. For effective transfer of load from one member to another there must be proper anchorage between members of composite material. In general, anchorage is achieved by a combination of bond (adhesion, friction and bearing against transverse ribs) and bearing on 90^0 and 180^0 hooks. Current code provisions (ACI 352R-02 (ACI– ASCE, 2002), IS 13920 (BIS, 1993) and IS 456 (BIS, 2000)) specify the development length of straight as well as hooked bars. Placement of these bars with large development lengths is the major problem at the exterior beam–column junctions. Use of high-strength steel makes this problem more critical. The bends and tails of the hooked bars create congestion, which hinders concrete placement and compaction inside the joint during casting; but concrete compressive strength is more important than the number of joint hoops to define shear capacity of the joint (Alva *et al.*, 2007). Some attempts by researchers have been made to minimize reinforcement congestion at the exterior beam– column joints. Use of steel plates for anchoring the longitudinal reinforcement of beams (Kotsovou and Mouzakis, 2011) minimised cracking and deformation of the joints. Use of steel fibre reinforcement concrete at the junction reduced the number of lateral ties without affecting ductility (Patel *et al.*, 2013). Headed bars can offer a potential solution to these problems and may also ease reinforcement laying, concrete placement and compaction (Chun *et al.*, 2007). To study the parameters influencing the behavior of mechanical anchorage, research was conducted on idealized evaluations where headed bars were pulled from concrete blocks (Wright and McCabe, 1997) and columns (Bashandy, 1996; Chun *et al.*, 2009). A compression–compression–tension (CCT) node test was conducted on beam specimens with headed bars; the variables being studied were angle of compression strut, head size and shape, bar diameter and confining effect (Thompson *et al.*, 2005). By using actual specimens of beam–column joints, the experimental work was conducted to assess the effectiveness of headed bars with the emphasis on joint detailing (Chun *et al.*, 2007; Wallace *et al.*, 1998) and small head size (Kang *et al.*, 2010).

2. OBJECTIVES

The objective of this study is to evaluate nonlinear performance of retrofitted exterior joint with PISA technique. Six types of different conventional and retrofitted anchorage system (using PISA technique) are modeled and analyzed by nonlinear finite element based ABAQUS program. The study program was conducted as per the following sequence.

- Modeling of six different configurations of conventional (group-A) and retrofitted (group-B) anchorage systems in exterior joints

- Conduct model analysis for effective location of supplementary anchorage.
- Post processing of joint models by nonlinear analysis against conventional and retrofitted modeled specimens of six different configurations of anchorage systems by using ABAQUS modeling
- Simulate the crack propagation and Damage index of six different types of modeled specimens.
- Validate the modeling results with experimental observations.

3. STUDY LIMITATIONS

This study is limited to conduct model analysis on integrated exterior beam-column joint under quasi-static load condition. Six different configurations of anchorage systems used in practice are considered for post retrofitting process. As per design the initial failure of conventional anchorage system was addressed in joint core that was retrofitted by PISA technique for relocation of plastic hinge mechanism in different anchorage systems. During this process, the post installation of supplementary anchorage was done by using headed bar as supplementary anchorage with adhesive bond fastening technique. The configuration of different anchorage systems are followed by Indian standard and American standard design codes with no lateral confinement of reinforcement in joint. Based on strut mechanism joint failure is analyzed by principal tensile stresses developed in conventional and retrofitted joint core.

4. MODELING OF ANCHORAGE SYSTEM

The detailing of anchorage system in six types of exterior joints representing conventional and retrofitted joints are shown in Fig1a-1b to Fig 6a-6b. The size of beam element was 150x250mm depth with extruded length (L_b) 750mm. The column size is 250x150 mm width and height (H_b) 1000mm. The configuration of anchorage systems are described by straight bar (Fig1a,1b), 90 degree bend (Fig2a,2b), 180 degree hook (Fig3a,3b- confirming to design code IS456:2000) and single head (Fig4a,4b), double head anchorage (Fig5a,5b)-confirming to ACI 318-19, ACI 352R-02) and anchorage of long 90 degree bend (Fig6a,6b) resembling ductile detailing (as per IS 13920-2016). The main reinforcement of modeled specimen consists of 12mm diameter HYSD bars 2nos both at top and bottom, confirming to yield strength 230MPa. Secondary reinforcement by lateral ties and stirrups 8mm diameter at 50mm c/c, and supplementary anchorage by square headed bar (head size 25x25mm and thickness 4mm) with 8mm shank diameter that was extended to full bond length of 200mm inside the beam. The ratio of head area (A_h) and bar (A_d) was kept more than 4 as per ACI 318-19 design guide lines.

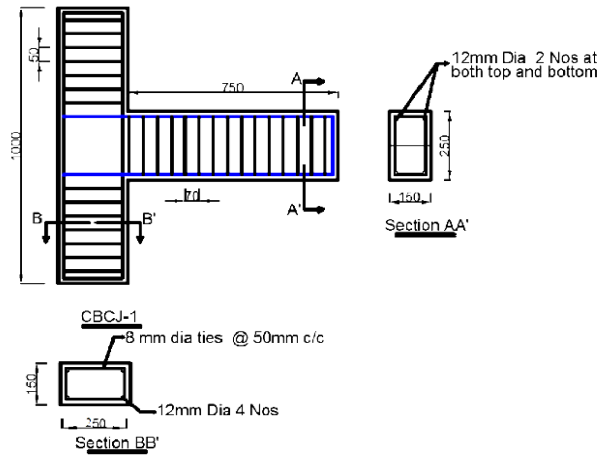


Fig 1a. Conventional Straight CBCJ-1

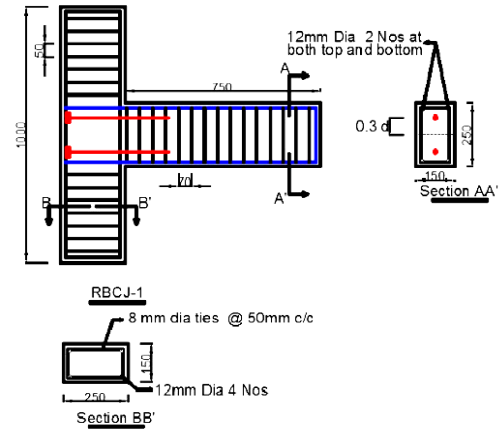


Fig 1b. Retrofitted Straight RBCJ-1

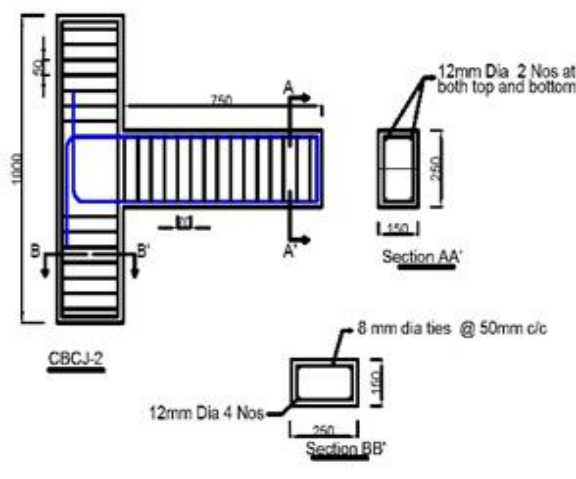


Fig 2a Conventional 90 Degree CBCJ-2

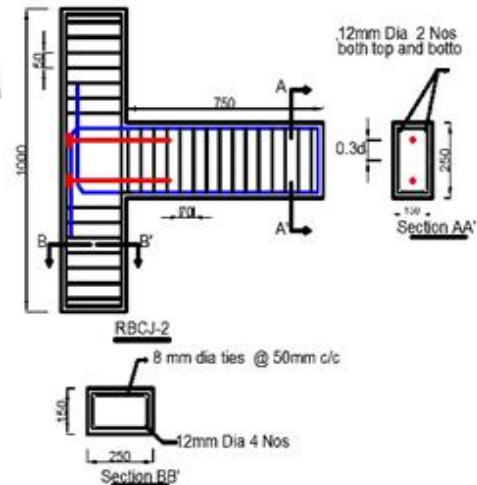


Fig2b: Retrofitted 90 Degree RBCJ-2

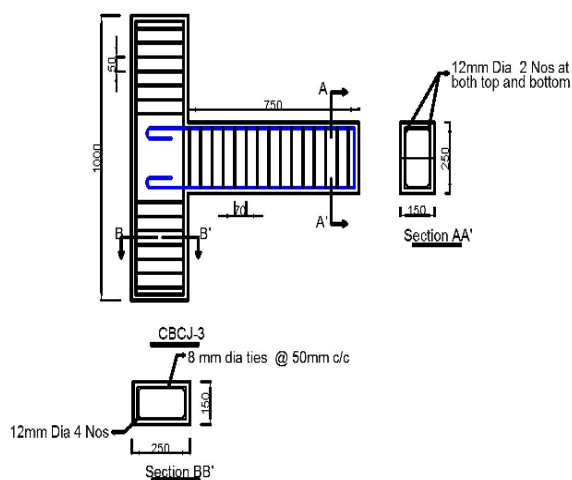


Fig 3a:Conventional 180° hook CBCJ-3

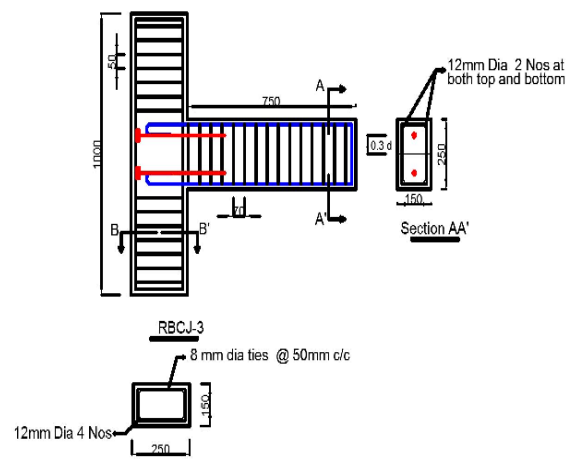


Fig 3b:Retrofitted 180° hook RBCJ-3

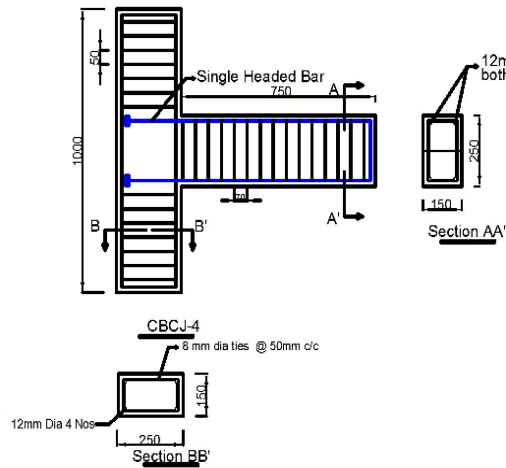


Fig 4a: Conventional Single Headed CBCJ-4

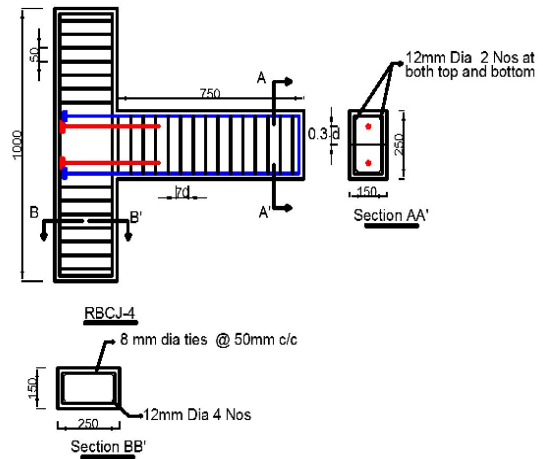


Fig 4b: Retrofitted Single Headed RBCJ-4

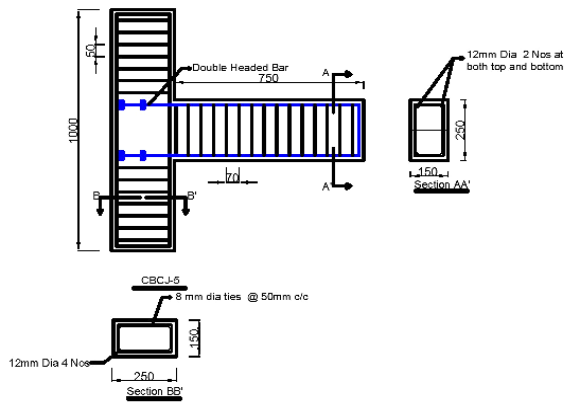


Fig 5a: Conventional Double Headed CBCJ-5

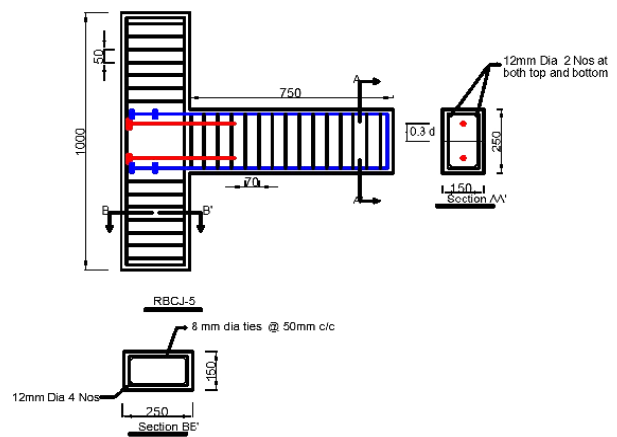


Fig 5b: Retrofitted Double Headed RBCJ-5

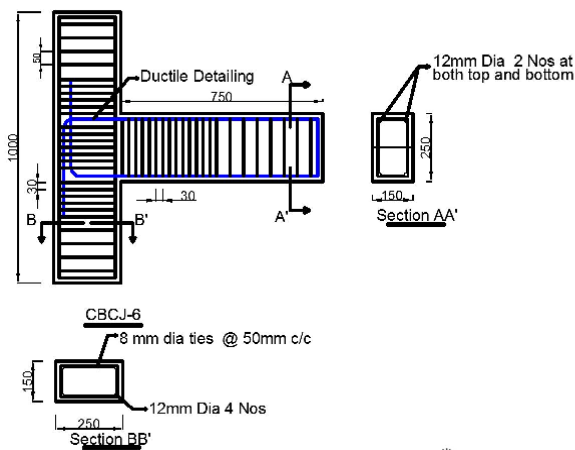


Fig 6a: Conventional Ductile Detailing CBCJ-6

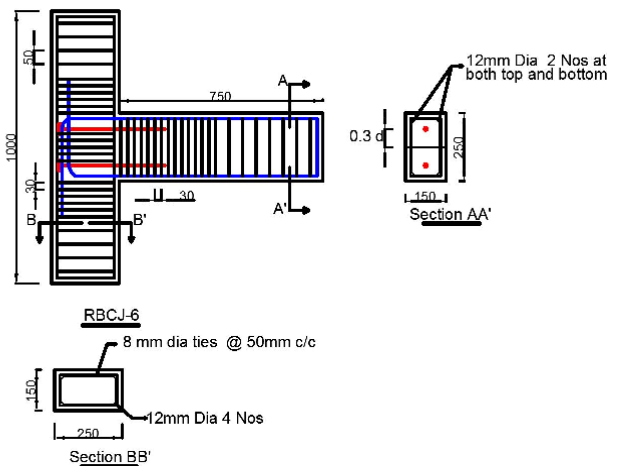


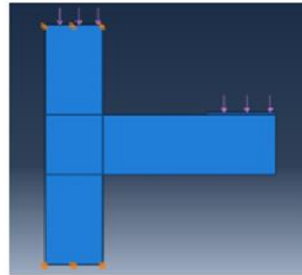
Fig 6b: Retrofitted Ductile Detailing RBCJ-6

5. ABAQUS Modeling

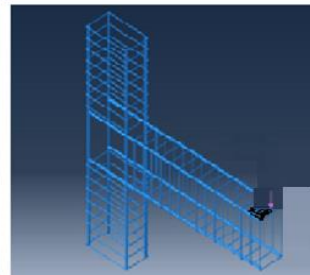
A nonlinear Finite Element Analysis (FEA) based ABAQUS software used to model the integrated

connection system of exterior joint and simulate the response of six different configurations of conventional and retrofitted anchorage systems under quasi static

loads. To perform numerical simulation of beam-column joint FEM-based software ABAQUS program was used to solve both elastic and inelastic performance under static loads. ABAQUS/CAE 6.14-1 VERSION



Modeling of concrete
Fig.7a



Modeling of reinforcement
Fig.7b

Reinforcement in beam and column are used 12mm diameter bar as main steel and 8mm diameter bar is used for stirrups in beam and 8mm tie bars are used in columns as mentioned in Figure 7a & 7b. Modeling of concrete was done by using 3D Solid element and steel by 2D wire element. The size of mesh 25x25mm. The material properties of concrete density 24000N/m³ and steel density 78500N/m³ are considered respectively. Mechanical Properties of Young's modulus of concrete E_c and steel E_s are 25000MPa and 2×10^5 MPa respectively. The interaction bond mechanism between concrete and steel is achieved by using EMBED region option which is an inbuilt option of ABAQUS program.

5.1 Concrete Damage Plasticity

The concrete damage plasticity (CDP) model was selected in the model analysis of beam-column joint by ABAQUS modeling. It shows wide spread potentiality for modeling of reinforced concrete and other quasi-brittle material in different types of RC structure. Many researchers applied CDP model for nonlinear performance of the beam-column joint. Additionally, it takes into account the isotropic damage elasticity concepts with isotropic tensile and compressive plasticity and considers the degradation of elastic stiffness produced by plastic strains both in compression and tension. The failure mechanism of this model assumes that both the tensile cracking and the compressive crushing and represents damage characteristics of the material.

Different parameters required in the CDP model were studied and selected based on available literature both for conventional as well as retrofitted specimens. The dilation angle for the model was taken as 36°. It is the angle obtained due to a change in volumetric strain produced due to plastic shearing. It depends on the angle of internal friction. Dilation angle controls the amount of plastic volumetric strain produced due to plastic shearing. Normally dilation angle is taken between 30° and 40° for concrete to avoid large variation between experimental work and

was used for modeling and analysis of beam-column joint. The size of beam dimension 150mm x 250 mm and column dimension 250mm x 150mm with 1000mm column height.

numerical modeling. For the seismic design of reinforced concrete, the value of dilation angle is normally between 35° to 38°. Moreover, eccentricity is the deviation from the center. The default value for eccentricity was taken, i.e., 0.1. If the value is increased by 0.1 the curvature of flow potential is increased. If the value is decreased from the default value, the convergence problem may occur if confinement pressure is not high enough. Furthermore, the ratio of biaxial loading (f_b) to uniaxial loading (f_{c0}) is normally taken as 1 or greater than 1. In this case default value was taken i.e., $f_b/f_{c0} = 1.16$. K is the shape factor and default value for $K = 0.667$. The viscosity parameter shows the amount of flow potential in a material. A lower viscosity parameter value is better as higher values result in a high force of reaction. Therefore, the viscosity parameter, in this case, is taken as 0.001.

Compressive and Tensile behavior of concrete was determined by using EN 1992 Eurocode 2: Design of concrete structures part 1-1. It describes different principles and requirements for the safety, serviceability, and durability of concrete structures with specific provisions of buildings. Eurocode 2 applies to the design of civil engineering works such as buildings, roads, bridges, etc. It is applied to plain, reinforced, and prestressed concretes. It complies with the specifications and requirements given in EN 1992-1-1 about safety, serviceability of the structures, the basis of their design, and verification of structures given in EN 1990; basis of structural design. The limitation of the Eurocode-2 for concrete structures is that it is concerned only with the requirements for resistance, safety, serviceability, durability, and fire resistance of the structures. Moreover, it does not consider the other requirements like thermal or sound insulation, etc.

5.2 Boundary Conditions

After the completion of assembly, a step was formed. In steps, a time period was provided for which the load is applied to the assembly. The load was then applied to the designated location according to the magnitude of the sample and boundary conditions were

hinge boundary conditions were applied, i.e., ($U_1 = U_2 = U_{R3} = 0$) at one end of column while roller support ($U_1 = U_{R2} = U_{R3} = 0$) at the other end in all specimens. “U” refers to translation motion while “UR” refers to rotation of the support. Both the boundary conditions for the column were studied and their effect on the strength and load values were observed.

5.3 Discretization of mesh

Meshing is the process of dividing the whole finite element model into a smaller number of chunks by the formation of different nodes at different points. Meshing is an important process as it allows us to apply load and find displacement or any other desired result at any point in the model. The greater the size of the mesh,

the smaller will be the number of iterations taken to analyze the whole model and vice versa. In a greater size mesh, a lesser number of nodes are formed, hence the number of iterations and time of analysis is reduced. In our case, the size of the mesh taken was 25 mm, and the element selected for concrete is C3D8R and steel is T3D2 truss element in improving the shear strength deformation against different structural loading. A monotonic load of 0 to 50 kN was applied at the end of the beam and 10 kN was applied on top of column for all specimens till the specimens reached the ultimate value. For application of load, Static general step was created for linear analysis, and Dynamic step was created for non linear analysis. Time period and increment values were given to all specimens.

CONCRETE DAMAGE PLASTICITY			
Concrete Compressive Behaviour		Concrete Compression Damage	
Yield Stress	Inelastic Strain	Damage Parameter	Inelastic Strain
10.2	0	0	0
12.8	7.74E-05	0	7.74E-05
15	0.000173585	0	0.000173585
16.8	0.000288679	0	0.000288679
18.2	0.000422642	0	0.000422642
19.2	0.000575472	0	0.000575472
19.8	0.00074717	0	0.00074717
20	0.000937736	0	0.000937736
19.8	0.00114717	0.01	0.00114717
19.2	0.001375472	0.04	0.001375472
18.2	0.001622642	0.09	0.001622642
16.8	0.001888679	0.16	0.001888679
15	0.002173585	0.25	0.002173585
12.8	0.002477358	0.36	0.002477358
10.2	0.0028	0.49	0.0028
7.2	0.003141509	0.64	0.003141509
3.8	0.003501887	0.81	0.003501887
Concrete Tensile Behaviour		Concrete Tension Damage	
Yield Stress	Cracking Strain	Damage Parameter	Cracking Strain
2	0	0	0
0.02	9.43E-04	0.99	9.43E-04

Fig. 8a: Concrete damage plasticity

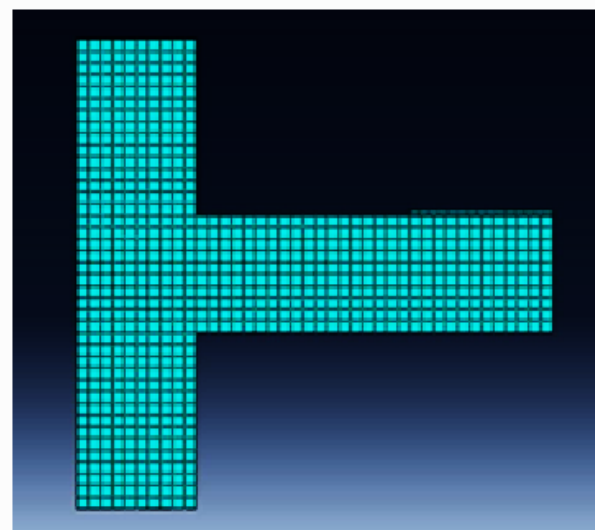


Fig 8b. Discretized mesh element

6. LOCATION OF SUPPLEMENTARY ANCHORAGE

Model analysis was conducted by ABAQUS software to identify the optimum location of supplementary anchorage for retrofitting of joints. Four

types of reinforcement joint models (A,B,C,D) representing different location of supplementary bar from neutral axis (Figure 9a) such as 0.3d,0.4d,0.5d and 0.1d respectively (d= effective depth) are analyzed.

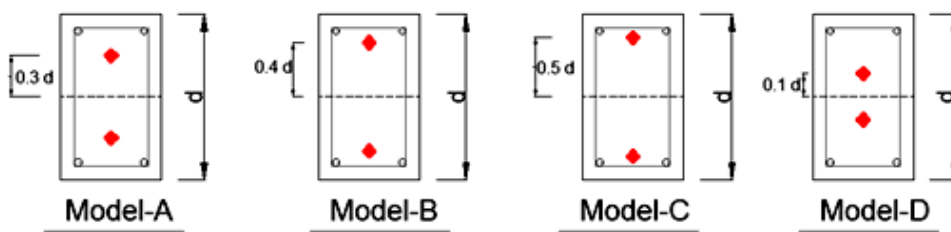


Fig 9a Models for optimum location of supplementary anchorage

The results shows Model-A (Fig10a), Model-B (Fig 10b), Model-C (Fig 10c), Model-D (Fig 10d) are representing stress values of 1.29MPa, 1.31Mpa, 1.32MPa, and 1.34MPa respectively. Model-A shows

least value of stress contours and was selected for location of supplementary anchorage during the retrofitting process. And the results are endorsed by ACI 318-2019 design provisions.

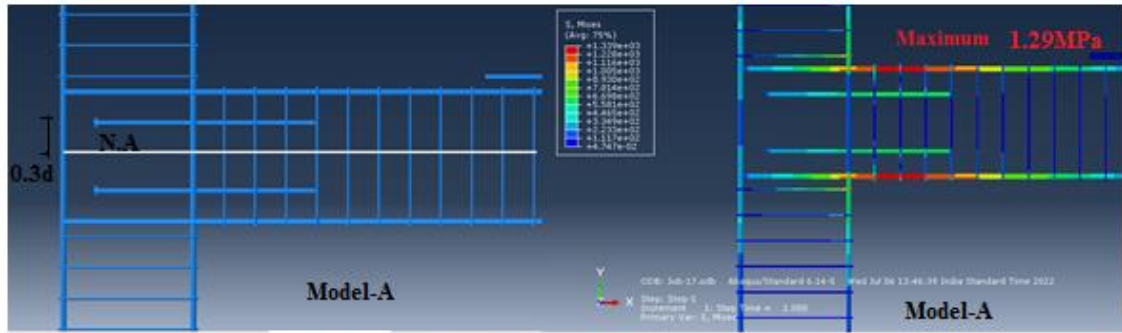


Fig 10a Stress analysis of Model-A

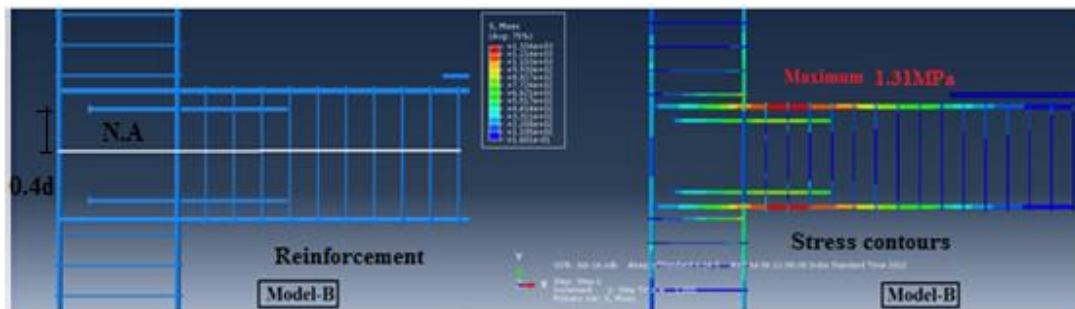


Fig 10b. Stress Analysis of model-B

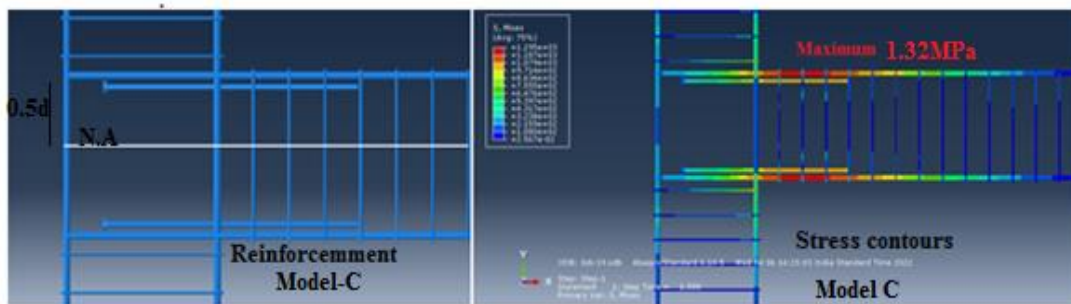


Fig 10c Stress Analysis of model-C

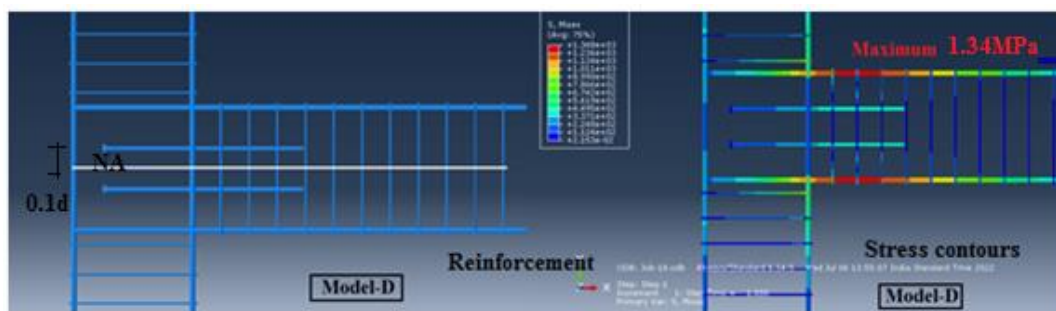


Fig 10 d. Stress Analysis of model-D

7. PARAMETRIC STUDY

The nonlinear parameters considered in the ABAQUS modeling study are aims to evaluate the failure mode and extent of damage in different conventional and retrofitted anchorage systems of joint models. The main parameters considered are Von Misses stress conditions, Principal tensile stress, Deflection, Moment rotation, Stiffness degradation and

Damage-T in joint core. The result shows considerable improvement in retrofitted anchorage system and shifting of plastic hinge mechanism from joint to beam region. Following observations were drawn.

7.1 Von-Mises stress condition

The Von-Mises stress conditions of joint concrete for both conventional and retrofitted modeled

specimens are shown in figures (Fig 11a, 11b-to-Fig 16a, 16b). The salient observations concludes that the conventional beam column joint of 90 degree bend (CBCJ2) experience more stress conditions (17.69MPa) than the rest of conventional anchorage specimens The conventional ductile bend (CBCJ6) shows minimum

stress (17.44) when compared with rest of conventional specimens. (Ref. Fig 17). Similarly the retrofitted beam column joint of 90 degree bend specimen (RBCJ2) shows maximum stress (17.31 N/mm²) and ductile bend of beam column joint specimen (RBCJ6) shows less stress (17.06 N/mm²) (Ref. Fig 17).

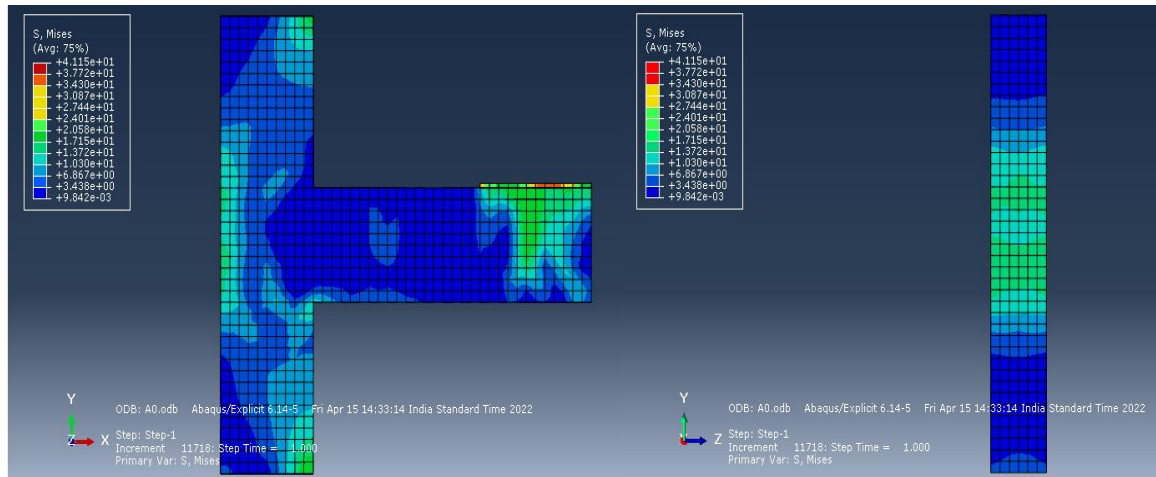


Fig 11a: Von Mises stresses in CBCJ-1 a) Elevation b) Side view

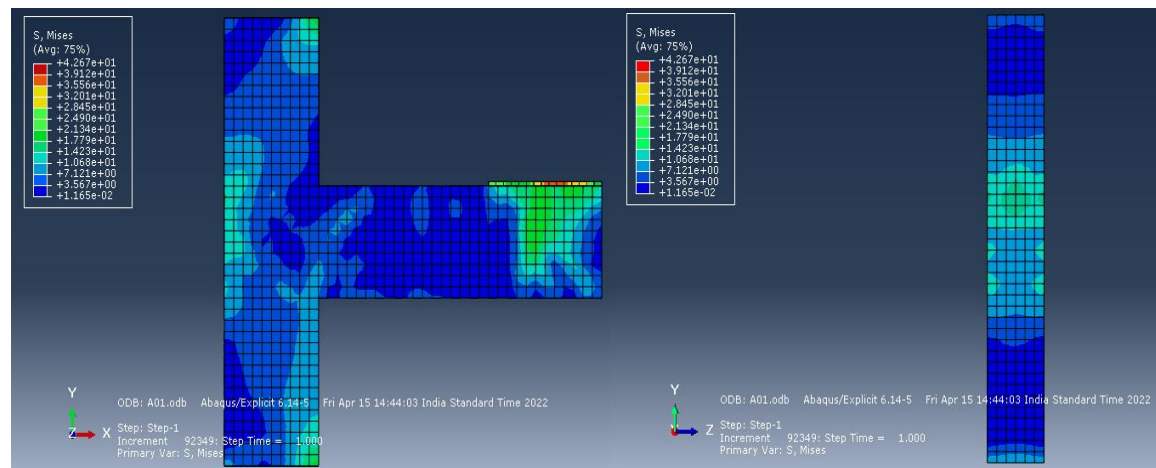


Fig 11b: Von Mises stress in RBCJ-1 a) Elevation b) Side view

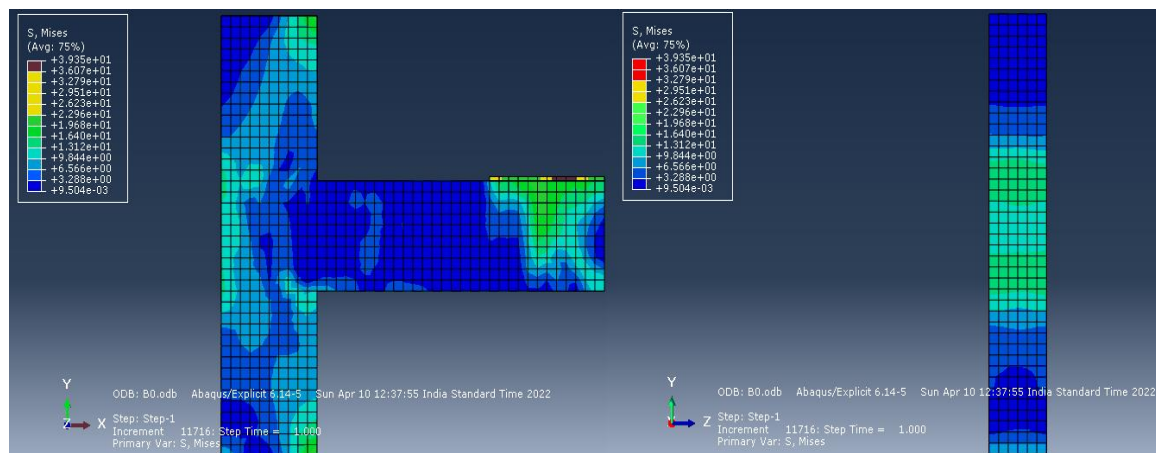


Fig 12a: Von Mises stress in CBCJ-2 a) Elevation b) Side view

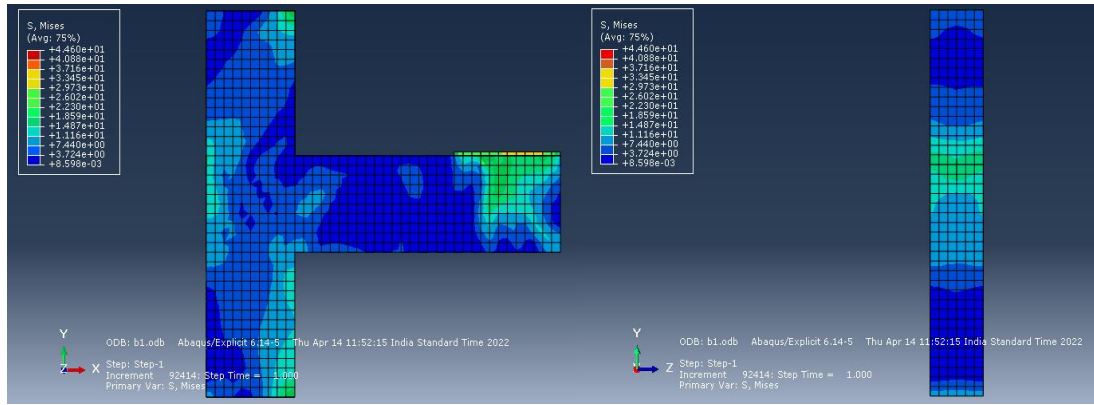


Fig 12b: Von Mises stress in RBCJ-2 a) Elevation b) Side view

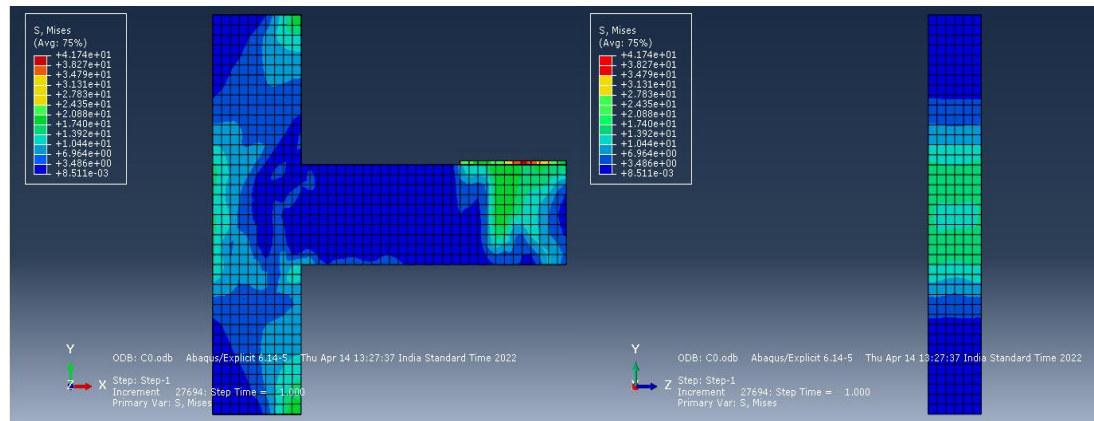


Fig 13a: Von Mises stress in CBCJ-3 a) Elevation b) Side view

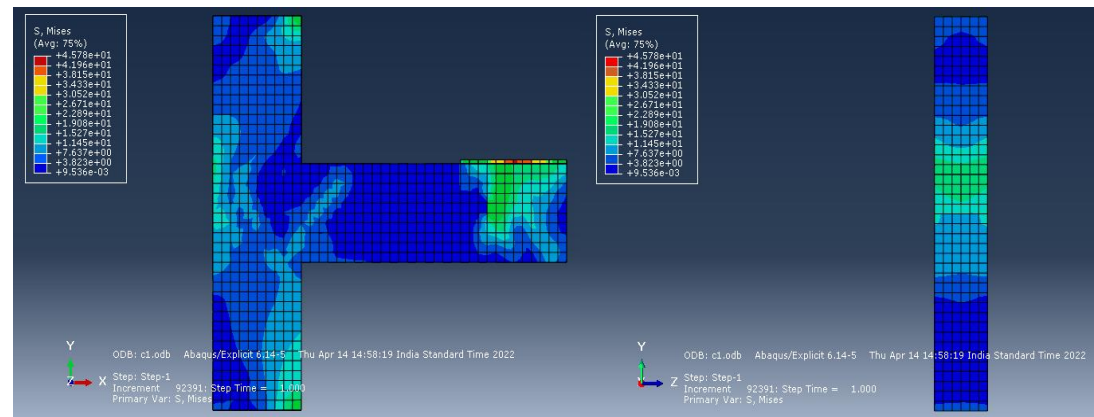


Fig 13b: Von Mises stress in RBCJ-3 a) Elevation b) Side view

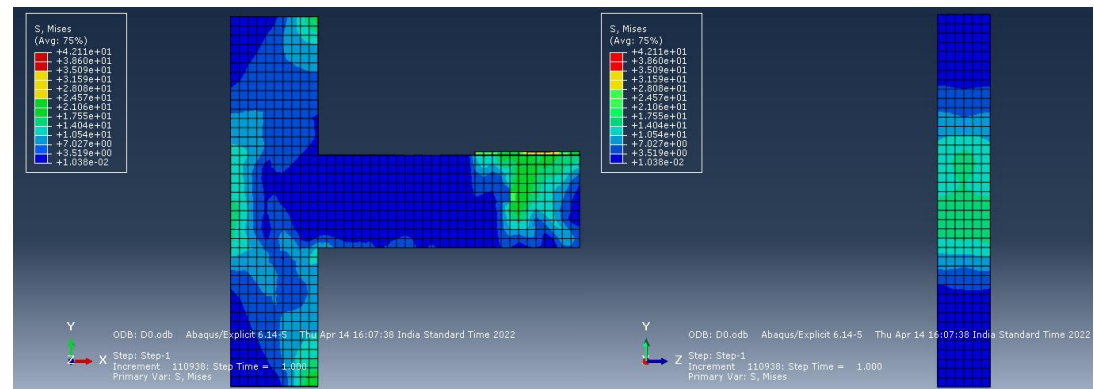


Fig 14a: Von Mises stress in CBCJ-4 a) Elevation b) Side view

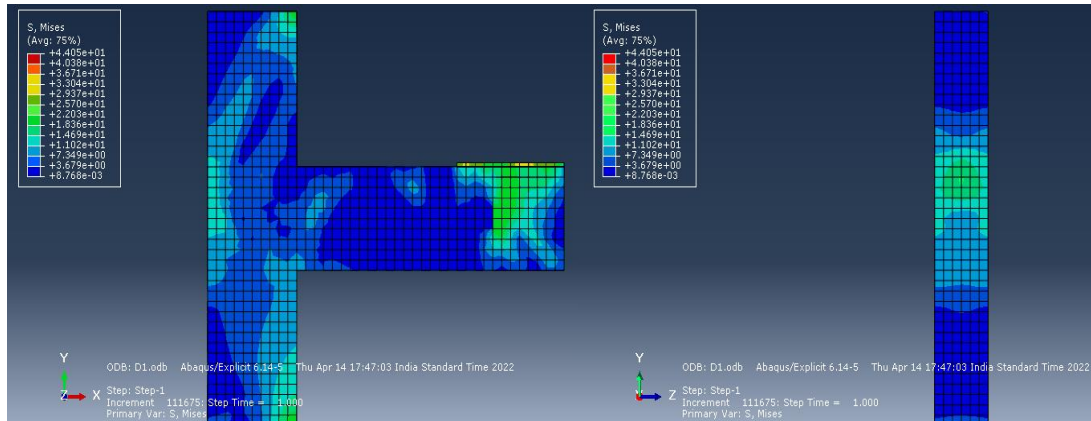


Fig14b: Von Mises stress in RBCJ-4 a) Elevation b) Side view

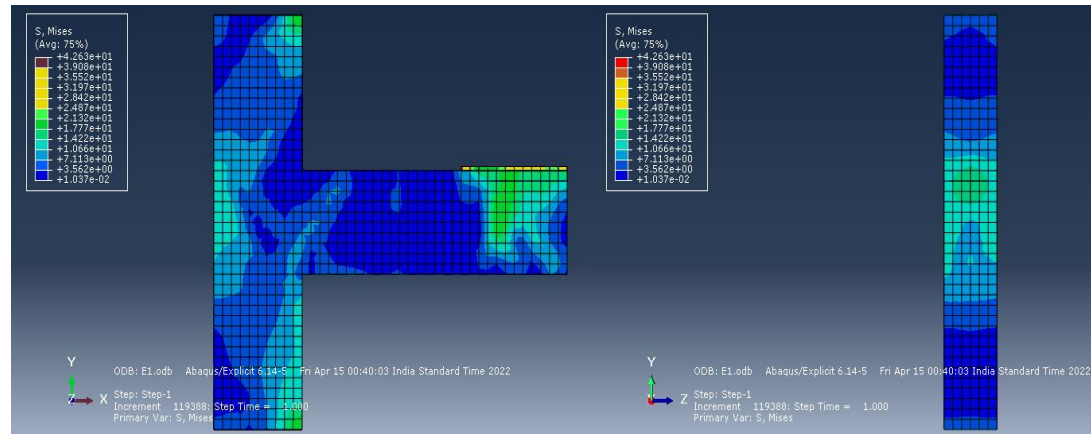


Fig 15a: Von Mises stress in CBCJ-5 a) Elevation b) Side view

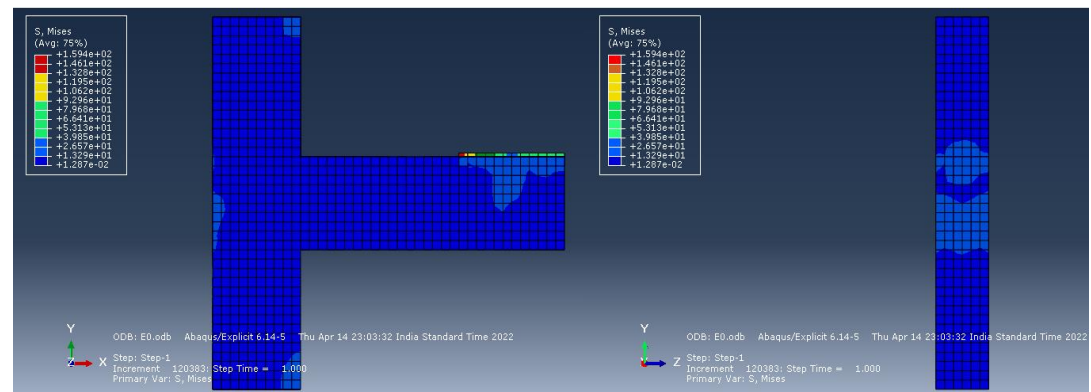


Fig 15b: Von Mises stress in RBCJ-5 a) Elevation b) Side view

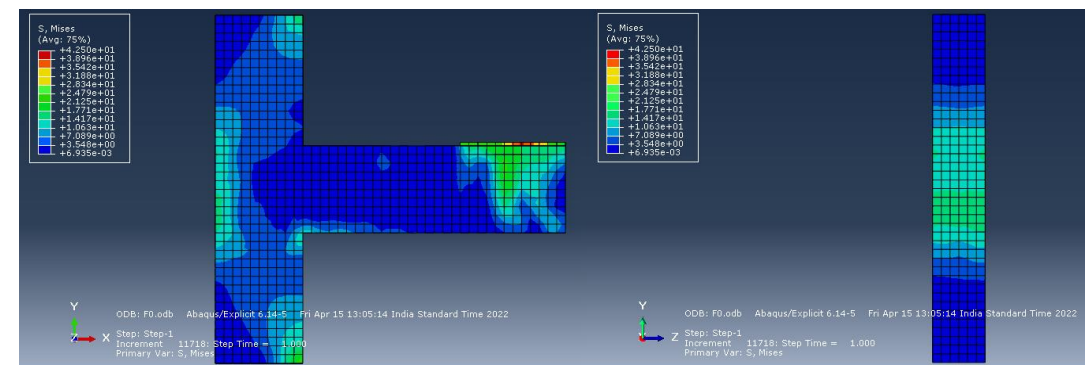


Fig16a: Von Mises stress in CBCJ-6 a) Elevation b) Side view

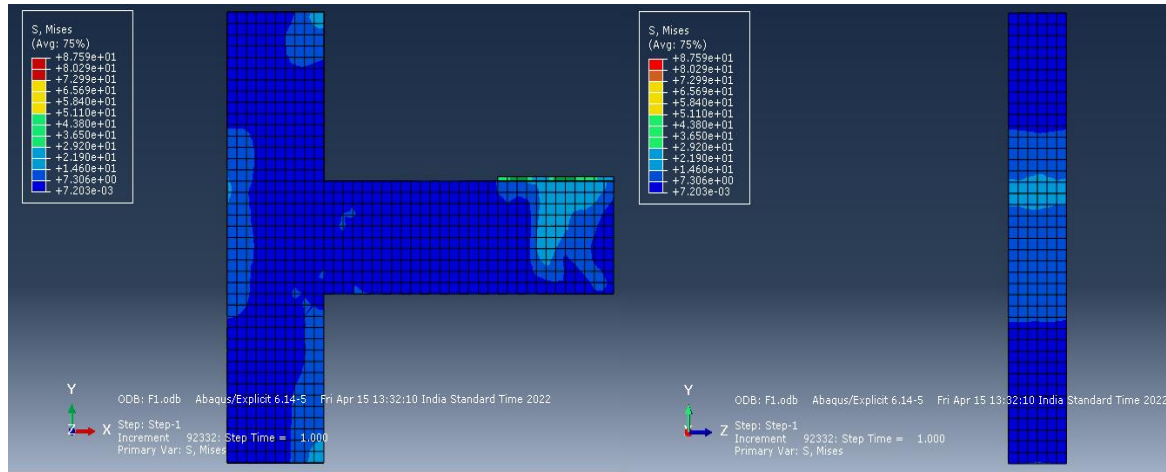


Fig 16b: Von Mises stress in RBCJ-6 a) Elevation b) Side view

7.2 Flexural stress in joint concrete

Flexural stresses in joint concrete was shown in Figure 17. It was observed that the flexural stresses in concrete was high in all types of conventional anchorage systems (Range 17.60-17.69) that was reduced by PISA retrofitting technique (Range 17.24-17.31). The decrease in stresses are between 2%-3% that was varied with configuration of anchorage systems. Observations of modeled stress contours in joint core revealed that all conventional anchorage systems (CBCJ1, CBCJ2, CBCJ3, CBCJ4, CBCJ6) shows more

concentrated stresses at joint that tends to more probable failure mode of joint except CBCJ5 (single headed bar) where the probability of failure mechanism diversified to at both joint core and beam. The subsequent observations of stress contours in retrofitted anchorage system revealed that all retrofitted joints (RBCJ1, RBCJ2, RBCJ3, RBCJ4, RBCJ5, RBCJ6) shows diversified stresses from joint core to beam due to presence of supplementary anchorage and the mechanism shifted to beam region from joint core.

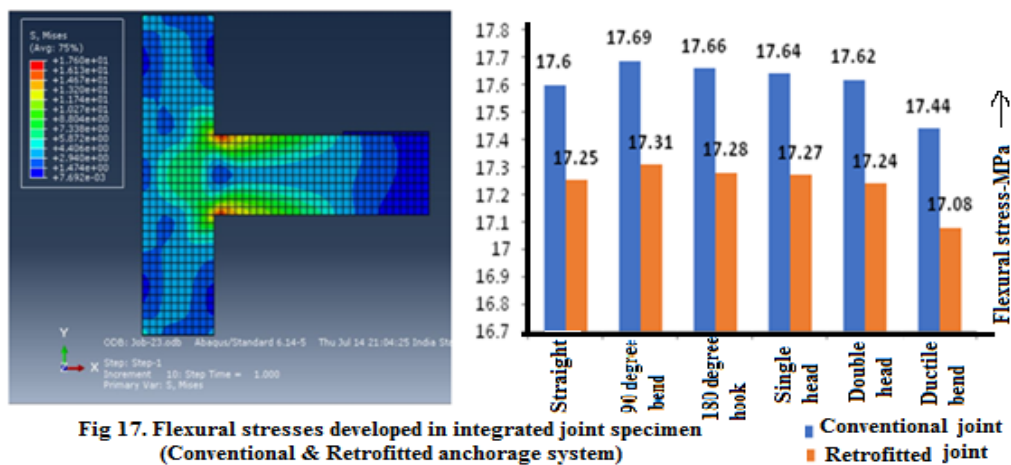


Fig 17. Flexural stresses developed in integrated joint specimen (Conventional & Retrofitted anchorage system)

7.3 Principal stresses in joint core

Maximum principal tensile stress in concrete evaluated from model analysis of different configurations of anchorage system. In general the cracks are appeared if principal stress exceed the limiting tensile stress of concrete. From the observations, conventional beam column joint with 90 degree bend (CBCJ2) shows high principal tensile stress of 1.867 N/mm². and conventional ductile bend (CBCJ6) shows minimum principal tensile stresses 1.850 N/mm when compared to all six specimens. The retrofitted beam column Joint of straight anchorage

(RBCJ1) shows maximum principal tensile stress of 1.82 N/mm² whereas ductile bend (RBCJ6) shows minimum principal tensile stress of 1.850 N/mm² from all six retrofitted specimens. Compared to conventional and retrofitted specimens, the presence of supplementary anchorage is decrease the principal tensile stress in retrofitted anchorage system and less cracks when compared to corresponding conventional models. Table1 shows the principal stress of conventional and retrofitted anchorage system in joint concrete.

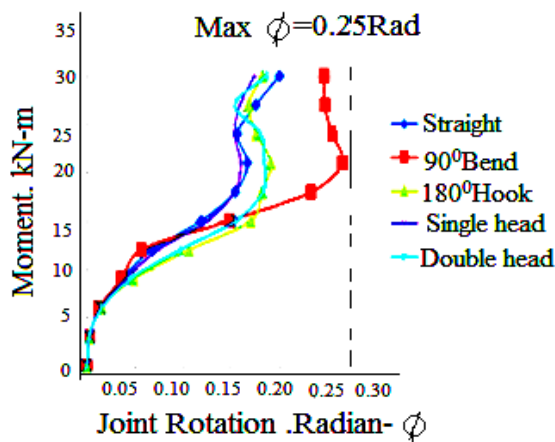
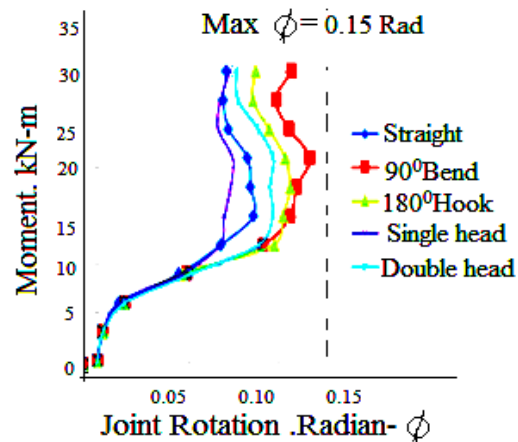
Table 1: Principal Tensile stress developed in different configuration of anchorage system

S. No	Specimen (Conventional anchorage)	Principal Tensile stress (MPa)	Specimen (Retrofitted anchorage)	Principal Tensile stress (MPa)
1	CBCJ1	1.860	RBCJ1	1.820
2	CBCJ2	1.867	RBCJ2	1.730
3	CBCJ3	1.853	RBCJ3	1.690
4	CBCJ4	1.852	RBCJ4	1.610
5	CBCJ5	1.851	RBCJ5	1.670
6	CBCJ6	1.850	RBCJ6	1.620

7.4 Joint-Rotation

The moment rotation of a joint was used to describe the connection system and energy absorption during its ultimate failure. Based on moment rotation the joint can be described as rigid or plastic. By using ABAQUS modeling program the joint rotation against the applied moments in various configurations of conventional and retrofitted anchorage systems are evaluated and shown in Fig 18a, Fig 18b. It is observed that more joint rotations and plastic hinge formations in conventional anchorage system when compared with successive retrofitted anchorage system. The maximum rotation of retrofitted joint decrease due to improvement of joint stiffness by presence of supplementary anchorage. It is observed that more rotations are in conventional specimens and less rotations retrofitted specimens. For the applied moment of 30 kN-m the observed rotation of 0.25 radian is in 90 degree bend

conventional anchorage system and less in single head anchorage system i.e. 0.15 radians. Similarly in Retrofitted specimens, 90 degree bend RBCJ2 shows high rotation of 0.1 radians whereas in single head anchorage system RBCJ5 shows less rotation of 0.07 radians. This indicates that retrofitted beam column joint with double headed bar allows shear deformation when compared with retrofitted beam column joint with 90 degree bend anchorage. Refer to Fig 18a, the conventional straight anchorage (CBCJ1), 90 degree bend (CBCJ2), 180 degree hook (CBCJ3) and double head (CBCJ5) anchorage systems shows more rotations (Greater than 0.15 Radian) and can be treated to show plastic hinge properties at ultimate failure (Ref Fig 18a). The corresponding retrofitted anchorage system of all anchorage systems shows rotation less than 0.015 Radians and can be treated as rigid connection system at ultimate failure (Ref Fig 18b).

**Fig 18a: Conventional anchorage****Fig 18b: Retrofitted anchorage**

7.5 Load-Deflection

In a structural system, stiffness is the major requirement part for strength and stability. The deflected values of beam end tip at constant load is shown in Table 2. The observed deflections of conventional model specimen CBJ6 shows less ductility as the deflection restricted to 1.369 mm, whereas the rest of anchorage systems shows consistent deflections of 1.372mm. Due to the increased stiffness, retrofitted anchorages of all anchorage systems shows less shear

deformation since the deflections are observed as 1.357mm. The deflection of retrofitted joint was 1.357mm that was less compared with conventional specimens. Refer to Table 3, there is a considerable improvement of yield load in all retrofitted anchorage system range between 9.93% to 22.80% when compared with conventional anchorage. The retrofitted double head anchorage system (RBCJ5) shows maximum increment of yield load and can be advised to use at higher elastic range or serviceability conditions.

Table 2: Load-Deflection

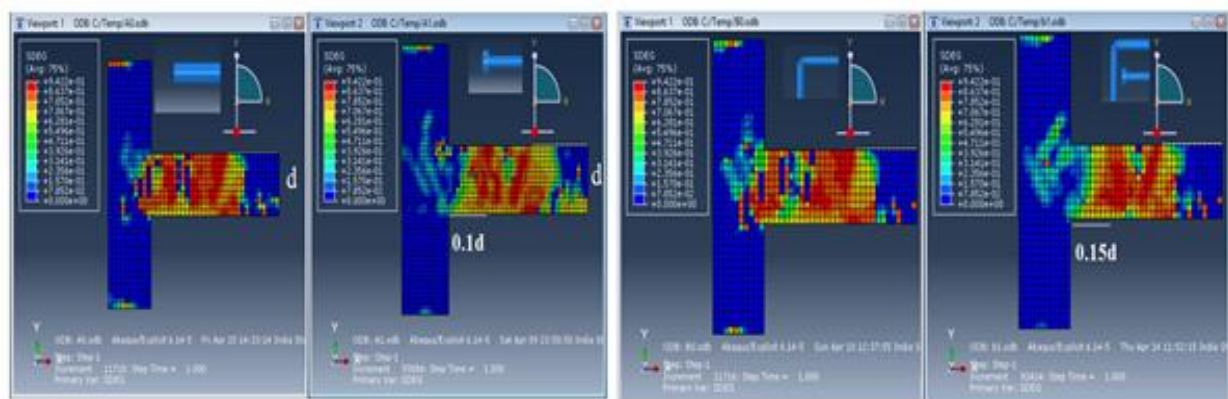
S. No	Specimen (Conventional anchorage)	Deflection @ beam end (mm)	Specimen (Retrofitted anchorage)	Deflection @ beam end (mm)	% Reduction
1	CBCJ1	1.372	RBCJ1	1.357	1.09
2	CBCJ2	1.372	RBCJ2	1.357	1.09
3	CBCJ3	1.373	RBCJ3	1.357	1.09
4	CBCJ4	1.372	RBCJ4	1.357	1.09
5	CBCJ5	1.372	RBCJ5	1.356	1.16
6	CBCJ6	1.369	RBCJ6	1.353	1.16

8. Degraded Stiffness

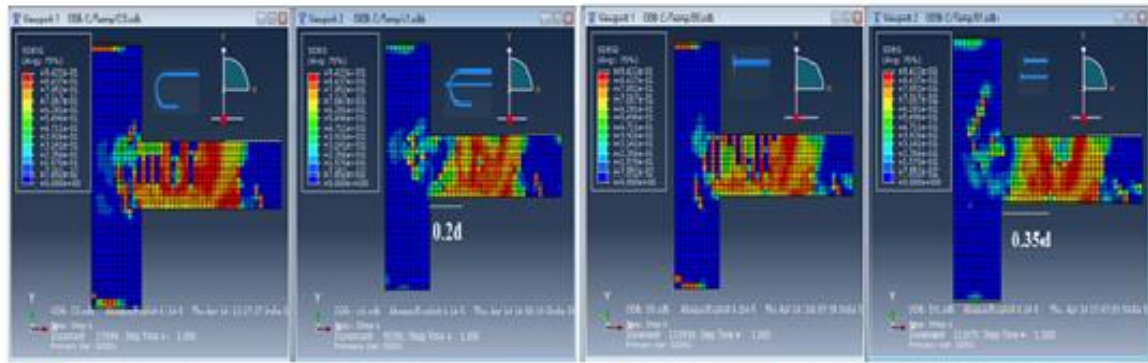
Stiffness degradation is a primer aspect from engineering design as it determines when fatigue cracks are more significant (Nicola Magino *et al* 2021). Gradual reduction of elastic stiffness can be described as the stiffness degradation in terms of tension and low confined compression state of concrete (Mazars *et al* 1984, Challamal *et al* 2005). Stiffness degradation and relocation of plastic hinge mechanism are the two important parameter that represents nonlinear behavior of concrete and failure mode. It is observed that plastic hinge is shifting from discrete joint region to discrete beam region and then to continuous beam region. Hardening stiffness is an important parameter that was used to define the behavior of plastic hinge after the yield point (Roohbakhsh & Sharma *et al.*, 2021). In straight anchorage system the stiffness degradation is more and the retrofitted straight anchorage system the stress contours are moving towards beam region. Similar behavior was observed in 90 degree bend anchorage system. In the 180 degree hook anchorage system the stress contours are more in discrete beam region when the same specimen is retrofitted the

contours are shifting towards beam region. The same behavior is observed in Single headed and Double headed anchorage systems. In ductile 90 degree bend specimens the stress contours are more in beam region and shifted further towards beam region if the supplementary headed anchorage system was used.

Fig 19a-to-Fig 19f shows the shifting of mechanical hinge formation from joint region to beam region in various configuration of retrofitted anchorage systems using PISA technique. The failure mechanism shifted from column face at 0.1d, 0.15d, 0.20d, 0.35d, 0.38d and 0.57d in retrofitted anchorage systems of straight bar (RBCJ1), 90 degree bend (RBCJ2), 180 degree hook (RBCJ3), single head (RBCJ4), double head (RBCJ5) and confined bend (RBCJ6) respectively. From the observations, the failure mode of conventional anchorage system (global failure) to local failure in retrofitted anchorage. Table.4 represents the typical failure mode of different retrofitted anchorage systems that was obtained from the modeling analysis.

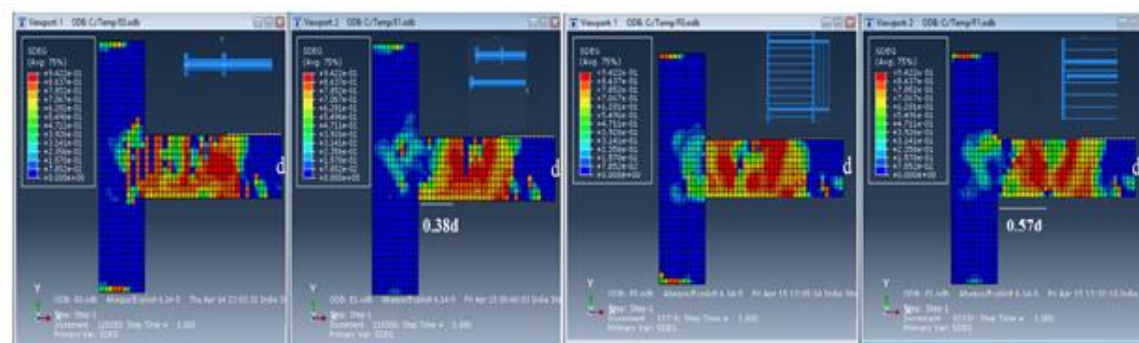


Conventional CBCJ-1 Retrofitted RBCJ-1 Conventional CBCJ-2 Retrofitted RBCJ-2
Fig 19a. Stress contours in straight anchorage Fig 19b. Stress contours in 90 degree bend



Conventional CBCJ-3 Retrofitted RBCJ-3 Conventional CBCJ-4 Retrofitted RBCJ-4

Fig 19c Stress contours 180 degree hook Fig.19d. Stress contours sigle head bar



Conventional CBCJ-5 Retrofitted RBCJ-5 Conventional CBCJ-6 Retrofitted RBCJ-6

Fig19e. Stress contours -Double head bar Fig 19f. Stress contours -Confined 90° bend

Table 3: Failure mode of anchorage systems

S. No	Configuration of anchorage system	Failure mechanics – Conventional Anchorage		Failure mechanics – Retrofitted Anchorage	
		Location	Failure mode	Location	Failure mode
1	Straight anchorage	Joint core	Global failure/ brittle mode	Discrete beam	Local failure/ brittle mode
2	90 degree bend	Joint core	Global failure/ brittle mode	Discrete beam	Local failure/ brittle mode
3	180 degree hook	Joint core	Global failure/ brittle mode	Discrete beam	Local failure/ ductile mode
4	Single head	Discrete beam	Local failure/ brittle mode	Discrete beam	Local failure/ brittle mode
5	Double head	Discrete beam	Local failure/ brittle mode	Flexural beam	Local failure/ ductile mode
6	Ductile bend	Discrete beam	Local failure/ brittle mode	Flexural beam	Local failure/ ductile mode

9. Crack mechanics- Failure mode

Conventional anchorage system of all configurations shows less number of cracks with large crack width in joint core that indicates brittle failure in joint region (Ref. Fig 20). Subsequently intensified

cracks are distributed in beam region with minimum crack width in all retrofitted anchorage system that indicates ductile failure. The load at which initial cracks appear in concrete ($W_{cr} > 0.3\text{mm}$) is considered as yield load.

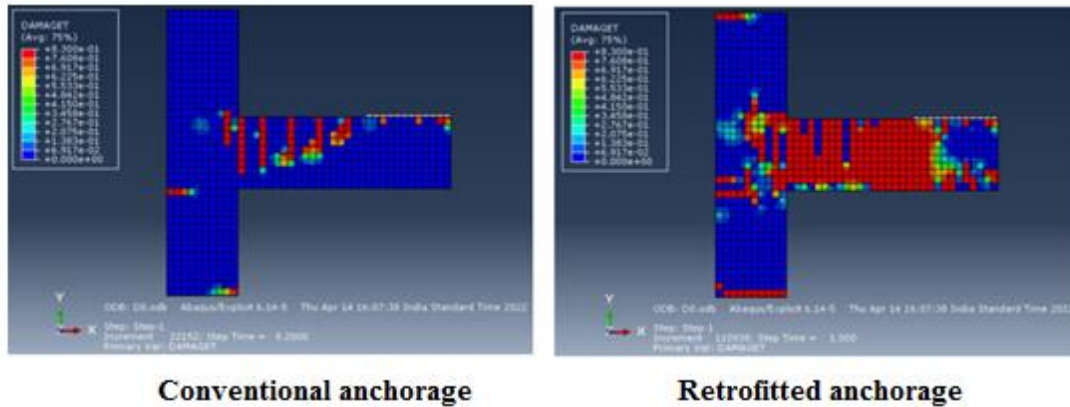


Fig20: Crack mechanics in Conventional & Retrofitted anchorage system (ABAQUS Model)

All six types of joint specimen and yield loads are tabulated and percentage of increase in load carrying capacity is calculated as shown in Table 4. The conventional straight anchorage system (CBCJ1) tends to shear failure in joint core that was shifted to column face of beam region in retrofitted anchorage system (RBCJ1). The global joint failure in straight anchorage tends to shift local beam brittle failure in straight anchorage system. The conventional 90 degree bend anchorage system (CBCJ2) tends to develop splitting tensile cracks in joint core that was transformed to beam region in retrofitted anchorage system (RBCJ2). The supplementary anchorage transformed global joint failure to local failure. The conventional 180 degree hooked anchorage system (CBCJ3) tends to develop shear and splitting tensile cracks in joint core that was transformed to splitting cracks in beam region with use of supplementary anchorage. Hence the global failure of CBCJ3 is transformed to local failure in RBCJ3

retrofitted anchorage system. The conventional single head anchorage system (CBCJ4) tends to develop splitting tensile cracks by cone of fracture at column face that was transformed to splitting tensile cracks in beam region by using supplementary anchorage. The local failure of CBCJ4 is further shifted to beam region in RBCJ4 retrofitted anchorage system. The conventional double head anchorage system (CBCJ4) tends to develop double cone of fracture by splitting tensile crack at discrete beam region was further shifted to flexural beam region with the use of supplementary anchorage. The local brittle failure of CBCJ5 in beam region was further shifted towards beam region and tends to happen ductile failure in RBCJ5 retrofitted anchorage system. Similarly the local brittle failure of CBCJ6 in beam region was further shifted towards beam region and tends to ductile failure in RBCJ6 retrofitted anchorage system.

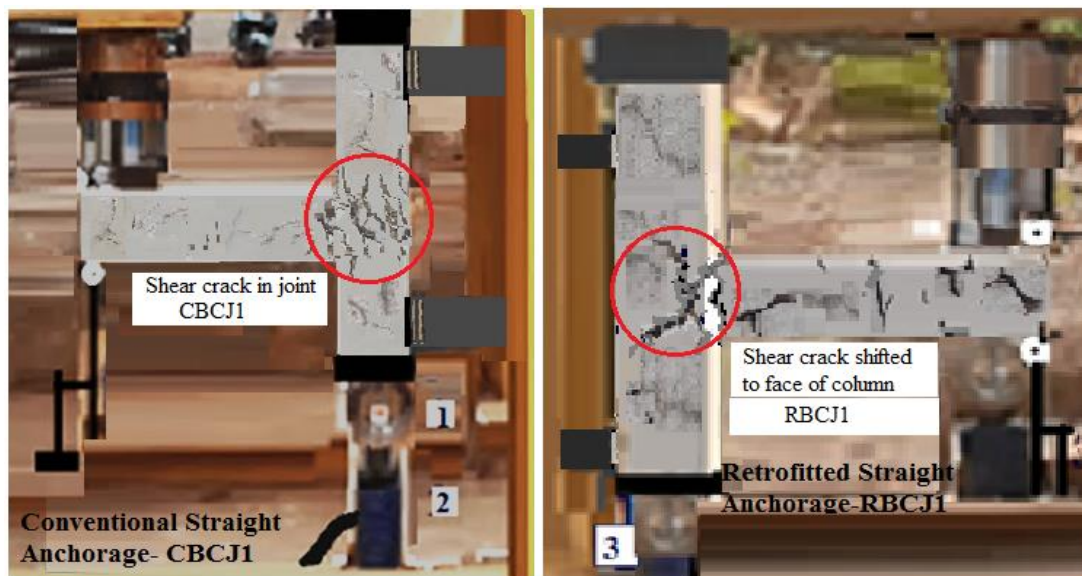


Fig.21 Crack pattern in Straight Conventional & Retrofitted Anchorage

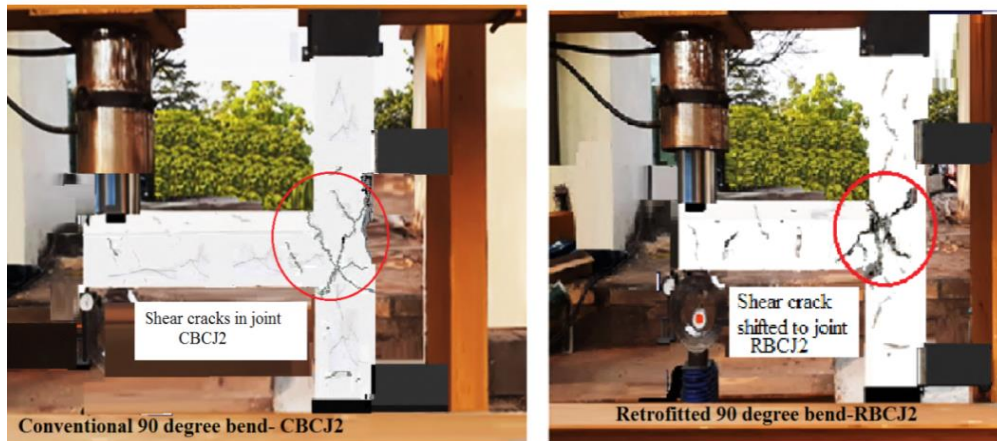


Fig 22. Crack pattern in 90 degree bend Conventional & Retrofitted Anchorage



Fig 23. Crack pattern in 180 degree hook .Conventional & Retrofitted anchorage

Fig 21 to Fig 23 shows experimental observations of crack pattern and shifting in conventional and retrofitted anchorage system of straight anchorage 90 degree bend, 180 degree hook.

The experiment test shows that joint failure of conventional anchorage causes global failure that was shifted to local failure in retrofitted anchorage.

Table 4: Yield load of different anchorage systems (ABAQUS model analysis)

S. No	Specimen (Conventional anchorage)	Yield load (kN)	Specimen (Retrofitted anchorage)	Yield load (k N)	(%) Increase of yield load
1	CBCJ1	28.250	RBCJ1	31.200	12.600
2	CBCJ2	29.120	RBCJ2	32.700	10.900
3	CBCJ3	29.450	RBCJ3	32.700	9.930
4	CBCJ4	29.670	RBCJ4	37.300	20.400
5	CBCJ5	32.500	RBCJ5	42.100	22.800
6	CBCJ6	34.600	RBCJ6	41.600	21.500

10. Validation of modeling results

The results of ABQUS modeling analysis were validated with experimental observations on typical exterior joint specimens of exterior beam column joint with three different configurations of straight anchorage, 90 degree bend and 180 degree hook retrofitted by PISA technique of same dimensions done by research studies of Padmanabham K & Jaydeep K @al (Table 5a, 5b –to-Table 7a, 7b).

The validation of results are presented in Table 11A & B, Table 12A & B and Table 13A & B respectively. Since the failure mechanism in joint core is mainly focused on development of principal tensile stress at ultimate loads, there is a good similarity between modeling and experimental results .The maximum variation of results in modeling and experimental results are presented in Table 5. It was noticed that the results of modeling analysis shows less value than experimental results and deviated between 8% to 16% in different configurations of anchorage systems.

Table 5a : Experimental results of Straight conventional anchorage

SLNo	Description	Applied Load	Deflection	Crack width	Moment @ joint	Joint Rotation	Column shear	Joint shear	Maximum Principle Stress@ joint
		(P) (kN)	δ (mm)	Wcr (mm)	(M) (kN-mm)	(θ) (Radian)	(Vc) (kN)	(Vj) (kN)	(Pt) (Mpa)
1	Initial load	0	0	0	0	0	0	0	0
2		10	2.70	0.12	7.50	0.003	8.75	33.15	0.1
3		20	6.24	0.26	15.00	0.008	17.5	66.31	0.37
4	Yield Load	28.64	9.70	0.31	21.00	0.012	25.06	94.959	0.67
5		30	11.68	0.58	22.50	0.015	26.25	99.46	0.73
6		40	19.12	1.43	30.00	0.020	35	132.62	1.14
7	Ultimate load	42.16	32.43	2.16	31.62	0.043	36.89	139.78	1.23
8	Load @ post failure	40	31.26	2.12	30.00	0.042	35	129.62	1.08
9		30	30.84	1.97	22.50	0.041	26.25	97.34	0.71

Table 5b Experimental Results of Straight Retrofitted anchorage system

SLNo	Description	Applied Load	Deflection	Crack width	Moment @ joint	Joint Rotation	Column shear	Joint shear	Maximum Principle Stress@ joint
		(P) (kN)	δ (mm)	Wcr (mm)	(M) (kN-mm)	(θ) (Radian)	(Vc) (kN)	(Vj) (kN)	(Pt) Mpa
1	Initial load	0	0	0	0	0	0	0	0
2		10	1.82	0.09	7.50	0.002	8.75	33.15	0.1
3		20	4.73	0.17	15.00	0.006	17.5	66.31	0.37
4	Yield Load	29.12	7.89	0.29	21.80	0.010	25.48	96.55	0.69
5		30	9.86	0.41	22.50	0.013	26.25	99.46	0.73
6		40	17.63	1.06	30.00	0.023	35	132.62	1.14
7	Ultimate load	44.36	31.84	1.81	33.27	0.042	38.85	147.08	1.33
8	Load @ post failure	40	30.57	1.74	30.00	0.040	35	128.62	1.09
9		30	29.93	1.71	22.50	0.039	26.25	93.46	0.61

The result of Table 10A shows a significant coincidence between experiment and model analysis. The percentage difference of principal stresses in various retrofitted anchorage systems range between 3%-16%. The model analysis results of retrofitted straight anchorage, 90 degree bend and 180 degree hook shows considerable similarity with experimental results (16.4%,3.35%,6.28%) as mentioned in Table 8. Both experimental and modeling studies are matched during relocation of plastic hinge mechanism (Ref: Fig 21, Fig 22, Fig 23) for the retrofitted joints. It was further identified that Straight bar and 90 degree bend anchorage system, shows the failures limiting in joint

core was successfully shifted to discrete region of beam at approximate 0.10d and 0.15d respectively (d: effective depth of beam) by using supplementary anchorage system. Similarly in 180 degree hook anchorage system, the initial failure happens near the face of column at 0.12d that was further shifted to 0.20d away from column face in retrofitting process. From the observation it may conclude that PISA technique helps to restrict global failure and transformed to local failure. The ABAQUS modeling addressed the failure in ideal conditions but still it meets the failure conditions of experimental testing.

Table 6a Experimental results of 90 degree bend anchorage

SLNo	Description	Applied Load	Deflection	Crack width	Moment @ joint	Joint Rotation	Column shear	Joint shear	Maximum Principle Stress@ joint
		(P) (kN)	δ (mm)	Wcr (mm)	(M) (kN-mm)	(θ) (Radian)	(Vc) (kN)	(Vj) (kN)	(Pt) Mpa
1	Initial load	0	0	0	0	0	0	0	0
2		10	2.44	0.09	7.5	0.0032	8.75	33.15	0.1
3		20	5.76	0.15	15.00	0.0077	17.5	66.31	0.37
4		30	10.52	0.29	22.50	0.0140	26.25	99.46	0.73
5	Yield Load	32.28	13.40	0.32	24.21	0.0161	28.24	107.02	0.821
6		40	19.63	0.68	30.00	0.0262	35	132.62	1.14
7	Ultimate load	48.13	32.28	1.94	36.09	0.0430	42.11	159.58	1.52
8	Load @ post failure	40	28.74	2.12	30.00	0.0382	35	123.62	1.09
9		30	27.96	2.03	22.50	0.0372	26.5	87.46	0.68

Table 6b Experimental results of Retrofitted 90 degree bend

SLNo	Description	Applied Load	Deflection	Crack width	Moment @ joint	Joint Rotation	Column shear	Joint shear	Maximum Principle Stress@ joint
		(P) (kN)	δ (mm)	W_{cr} (mm)	(M) (kN-mm)	(θ) (Radian)	(Vc) (kN)	(Vj) (kN)	(Pt) (Mpa)
1	Initial load	0	0	0	0	0	0	0	0
2		10	1.40	0.05	7.50	0.0018	8.75	33.15	0.1
3		20	3.57	0.12	15.00	0.0047	17.5	66.31	0.37
4		30	6.52	0.23	22.50	0.0087	26.25	99.46	0.73
5	Yield Load	36.24	9.16	0.29	25.96	0.0122	31.17	120.15	0.98
6		40	16.12	0.66	30.00	0.0215	35	132.62	1.14
7		50	21.48	0.94	37.50	0.0286	43.75	165.78	1.59
8	Ultimate load	57.32	27.18	1.82	43.00	0.0362	47.11	179.90	1.79
9	Post failure	50	26.43	1.97	37.50	0.0335	43.75	136.78	1.46
10		40	28.52	1.91	30.00	0.0335	35	121.32	1.02

Table 7a. Experimental results of conventional 180 degree hook

SLNo	Description	Applied Load	Deflection	Crack width	Moment @ joint	Joint Rotation	Column shear	Joint shear	Maximum Principle Stress@ joint
		(P) (kN)	δ (mm)	W_{cr} (mm)	(M) (kN-mm)	(θ) (Radian)	(Vc) (kN)	(Vj) (kN)	(Pt) (Mpa)
1	Initial load	0	0	0	0	0	0	0	0
2		10	2.47	0.06	7.50	0.001	8.75	33.15	0.1
3		20	5.3	0.12	15.00	0.001	17.5	66.31	0.37
4		30	9.34	0.23	22.50	0.002	26.25	99.46	0.73
5	Yield Load	38.24	13.23	0.29	28.79	0.002	33.46	126.78	1.06
6		40	15.75	0.66	30.00	0.002	35	132.62	1.14
7		50	21.68	0.94	37.50	0.003	43.75	165.78	1.59
8	Ultimate Load	58.37	28.46	1.82	45.00	0.005	51.07	193.53	1.98
9	Post Failure	60	31.58	1.97	46.78	0.005	52.5	198.93	2.06
10		50	30.82	2.14	45.00	0.00	51.07	165.78	1.59
		40	28.41	2.11	37.50	0.0397	35	132.62	1.14

Table 7b. Experimental results of Retrofitted 180 degree hook

SLNo	Description	Applied Load	Deflection	Crack width	Moment @ joint	Joint Rotation	Column shear	Joint shear	Maximum Principle Stress@ joint
		(P) (kN)	δ (mm)	W_{cr} (mm)	M (kN-mm)	(θ) (Radian)	(Vc) (kN)	(Vj) (kN)	(Pt) (Mpa)
1	Initial load	0	0	0	0	0	0	0	0
2		10	1.43	0.05	7.50	0	8.75	33.15	0.1
3		20	3.82	0.09	15.00	0	17.5	66.31	0.37
4		30	6.54	0.14	22.50	0.001	26.25	99.46	0.73
5		40	9.18	0.23	30.00	0.002	35	132.62	1.06
6	Yield Load (from graph)	41.7	9.53	0.30	31.24	0.002	36.44	138.09	1.21
7		50	15.62	0.83	37.5	0.003	43.75	165.78	1.59
8		60	23.27	1.25	45	0.003	52.5	196.28	2.02
9	Ultimate Load	60.52	30.02	1.66	52.5	0.004	51.8	198.28	2.06
10		50	27.83	1.97	55.5	0.005	43.75	124.32	1.59
11		40	26.41	2.02	52.5	0.005	35	123.48	1.14

Table.8 Comparison of Principal stress in joint core

S.No	Configuration of Anchorage	A Experimental Results (MPa)	B Modelling Results (MPa)	Percentage difference (A&B)
1	Conventional Straight Anchorage system	1.23	1.86	8.29
2	Retrofitted Straight Anchorage system	1.33	1.82	16.4
3	Conventional 90 Degree Bend Anchorage system	1.52	1.87	15.37
4	Retrofitted 90 Degree Bend Anchorage system	1.79	1.73	3.35
5	Conventional 180 Degree Hook Anchorage system	2.06	1.853	10.04
6	Retrofitted 180 Degree Hook Anchorage system	1.59	1.69	6.28

11. SUMMARY & CONCLUSION

PISA technique endorsed as successful retrofitting measure of RC exterior beam-column joint. This technique can be applied to various anchorage systems of exterior joint with viable construction practice. Performance evaluation of exterior joint using supplementary anchorage system shows reduced crack width, delay of post cracking phenomena, and shifting of plastic hinge mechanism from joint region to beam region. This properties are significantly influence the failure mode of integrated joint system. Also the failure mechanics helps to transform the joint from global failure to local failure. Hence PISA technique can be addressed to meet the retrofitting measures for rehabilitation of beam-column joint. Following observations are noted

1. Post Cracking behavior of joint is effectively controlled by PISA technique. The developed principal tensile stresses in joint core are reduced in retrofitted anchorage systems.(Range:2.15%-13.36%).
2. Confined boundaries, uniform stress distribution and node formation under stable equilibrium conditions are the key parameters that reduce principal tensile stresses in all types of anchorage systems by implementation of supplementary anchorage . The maximum reduction 13.3% was observed in RBCJ-6.
3. All retrofitted anchorage systems shows considerable improvement of its capacity with the use of supplementary anchorage. The minimum load increment (9.93%) attained in 180 degree hook anchorage system (RBCJ-3) and maximum load increment (22.8%) and 25.6% that was observed in (RBCJ-5) double head bar and ductile detailed bend (RBCJ-6) respectively.
4. Von misses stresses in joint concrete was reduced in all configuration of retrofitted anchorage systems The range of reduction was between by 2.15 % - 2.83 % .The maximum and minimum reduction of 2.17% and 1.98 % was found in double headed and straight retrofitted anchorage system respectively
5. Relocation of plastic hinge mechanism is a crucial aspect that significantly influence the failure mechanics of a joint. A considerable shifting of plastic hinge mechanism was observed in all types of retrofitted anchorage system that changes brittle to ductile failure .The plastic hinge shifted from 0.10 d to 0.58 d (d: effective depth of beam) from the column face towards beam with use of PISA technique. In this context no research work was established so far.
6. The retrofitted anchorage systems of RBCJ4 ,RBCJ5, RBCJ6, shows significant improvement during post cracking performance and shifted the mechanism shifted to 0.10d,0.15d,0.0.20d respectively .This indicates a clear shifting of global failure mode to local failure with ductile mode .

12. FUTURE SCOPE

Future scope of this study may be extended to evaluate PISA retrofitting technique under reverse cyclic loads. The seismic vulnerability of beam-column joints are more susceptible and causes brittle failure by high shear conditions. Modeling and experimental analysis are required for implicit strengthening of RC exterior beam-column joint.

REFERENCES

- Mitra, N. (2007). An analytical study of reinforced concrete beam-column joint behavior under seismic loading. Ph.D. thesis. Department of Civil and Environmental Engineering, University of Washington.
- Fardis, M. N. (2004). A European perspective to performance-based seismic design, assessment and retrofitting. Proceedings of International workshop performance-based seismic design concepts and implementation. Bled, Slovenia, 28 June–1 July 2004.
- Pagni, C. A., & Lowes, L. N. (2004). Tools to enable prediction of the economic impact of earthquake damage in older RC beam-column joints. In: Proceedings of international workshop: performance-based seismic design concepts and implementation. Bled, Slovenia, 28 June–1 July 2004.
- Paulay, T., & Priestley, M. N. (1992). *Seismic design of reinforced concrete and masonry buildings* (Vol. 768). New York: Wiley.
- Birely, A. C., Lowes, L. N., & Lehman, D. E. (2012). A model for the practical nonlinear analysis of reinforced-concrete frames including joint flexibility. *Engineering Structures*, 34, 455-465.
- Pantazopoulou, S., & Bonacci, J. (1993). Consideration of questions about beam-column joints. *Structural Journal*, 89(1), 27-36.
- Pampanin, S., Calvi, G. M., & Moratti, M. (2002). Seismic behaviour of R.C. beam-column joints designed for gravity loads. 12th European conference on earthquake engineering, London, Paper no. 726.
- NTC. (2008). Ministero delle Infrastrutture (2008). DM 14 gennaio 2008, Norme Tecniche per le Costruzioni.
- Qualification of Post-Installed Adhesive Anchors in Concrete, American Concrete Institute, 2019
- El-Metwally, S. E., & Chen, W. F. (1988). Moment-rotation modeling of reinforced concrete beam-column connections. *Structural Journal*, 85(4), 384-394.
- Alath, S., & Kunnath, S. K. (1995). Modeling inelastic shear deformation in RC beam-column joints. In: Tenth conference on engineering mechanics. Boulder: University of Colorado; p. 822-825.
- Uma, S. R., & Prasad, A. M. Analytical modeling of RC beam-column connections under cyclic load.

- In: Eleventh world conference on earthquake engineering, Acapulco, Mexico.
- Kunnath, S. K. (1998). Macromodel-based nonlinear analysis of reinforced concrete structures. Structural engineering worldwide. Paper no. T101-5. Elsevier Science, Ltd., Oxford, England.
 - Anderson, M., Lehman, D., & Stanton, J. (2008). A cyclic shear stress-strain model for joints without transverse reinforcement. *Engineering Structures*, 30(4), 941-954.
 - Ghobarah, A., & Biddah, A. (1999). Dynamic analysis of reinforced concrete frames including joint shear deformation. *Engineering Structures*, 21(11), 971-987.
 - Elmorsi, M., Kianoush, M. R., & Tso, W. K. (2000). Modeling bond-slip deformations in reinforced concrete beam-column joints. *Canadian Journal of Civil Engineering*, 27(3), 490-505.
 - Youssef, M., & Ghobarah, A. (1999). Strength deterioration due to bond slip and concrete crushing in modeling of reinforced concrete members. *Structural Journal*, 96(6), 956-966.
 - Shin, M., & LaFave, J. M. (2004). Modeling of cyclic joint shear deformation contributions in RC beam-column connections to overall frame behavior. *Structural Engineering and Mechanics*, 18(5), 645-670.
 - Tajiri, S., Shiohara, H., & Kusuvara, F. A new macroelement of reinforced concrete beam column joint for elasto-plastic plane frame analysis. In: Eighth national conference of earthquake engineering, San Francisco, California.
 - Lowes, L. N., Mitra, N., & Altoontash, A. (2003). A beam-column joint model for simulating the earthquake response of reinforced concrete frames. Berkeley: Pacific Earthquake Engineering Research Center University of California.
 - Altoontash, A., & Deierlein, G. D. A versatile model for beam-column joints. In: ASCE structures congress, Seattle, WA.
 - Lowes, L. N., & Altoontash, A. (2002). Modeling the response of reinforced concrete beam-column joints. *Journal of Structural Engineering*, 1686-1697.
 - Mitra, N., & Lowes, L. N. (2007). Evaluation, calibration, and verification of a reinforced concrete beam-column joint model. *Journal of Structural Engineering*, 133(1), 105-120.
 - Jeon, J. S., Lowes, L. N., DesRoches, R., & Brilakis, I. (2015). Fragility curves for non-ductile reinforced concrete frames that exhibit different component response mechanisms. *Engineering Structures*, 85, 127-143.